TEKA. COMMISSION OF MOTORIZATION AND ENERGETICS IN AGRICULTURE – 2012, Vol. 12, No. 2, 291–296

Load of the kinematic pair piston-cylinder block in an axial piston pump

Tadeusz Zloto, Piotr Stryjewski

Institute of Mechanical Technologies, Czestochowa University of Technology

Summary. The paper presents an analysis of the load of the kinematic pair piston-cylinder block in an axial piston pump. The analysis was carried out by means of a spatial models of discrete and analog piston load. The value of reaction and friction forces occurring between the piston and cylinder block were determined for a typical axial piston pump. The load simulation was performed by means of the Mathcad software [15].

Key words: axial piston pump, piston load.

INTRODUCTION

Axial piston pumps have numerous industrial applications due to their ability to work with high pressures and high powers, as well as high efficiency understood as a ratio of power to mass or volume [11,12,20]. This type of displacement machines is most often employed in the drives of complex machines with high efficiency requirements [19,24]. This motivates continuous research on how to further improve exploitation parameters and modernize construction of these pumps.

The most important applications of hydraulic piston pumps include products of the companies Parker, Bosch-Rexroth and others, mostly in the following fields:
- aviation industry (airplanes),
- automotive industry (presses, numerical control machine tools, injection molding machines),
- heavy industry (pressure foundries, rolling mills, cokeries),
- building industry (excavators, loaders, extension arms),
- agriculture and forestry machines (forest cranes, elevators, drill rigs, mowers, combine-harvesters),
- military roadway systems (multifunction vehicles, building bridges).

One of the most popular types of piston machines with axial pistons are axial piston pumps with a sloping swash plate (Fig. 1) [1,3,5,7,10,14,16,17,18,22]. The cylinder block 4 rotates with the pistons 2, and the valve plate 9 and the swash plate 5 are stationary. By varying the inclination angle of the swash plate, the path of the

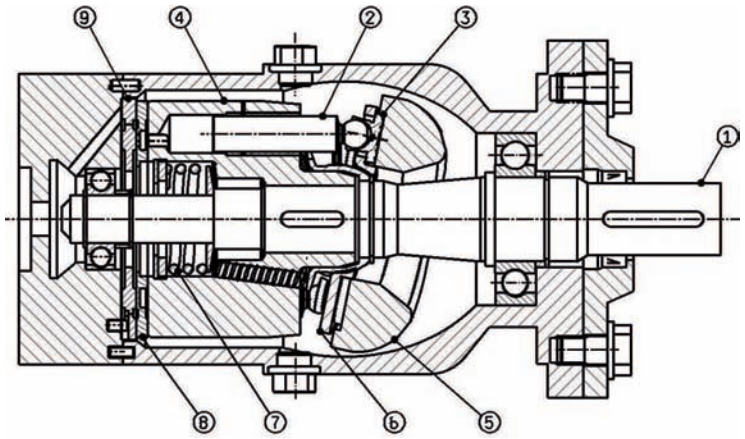

Fig. 1. The main elements of the axial piston pump: 1 – shaft, 2 – piston, 3 – slipper, 4 – cylinder block, 5 – swash plate, 6 – retainer plate , 7 – central spring, 8 – valve plate of the cylinder block, 9 – valve plate [11]

pistons is affected in their to-and fro motion and at the same time the flow intensity of the operating liquid varies.

Energy losses in axial piston pumps are most often caused by the operation of the kinematic pair piston-cylinder block.

ANALYSIS OF PISTON LOAD BY MEANS OF THE DISCRETE AND ANALOG MODELS

One of the characteristic features of the operation of the piston-cylinder block system in axial piston pumps with a sloping swash plate is that the hydrostatic slipper is acted upon by the radial force originating from pressure force. (Fig. 2).

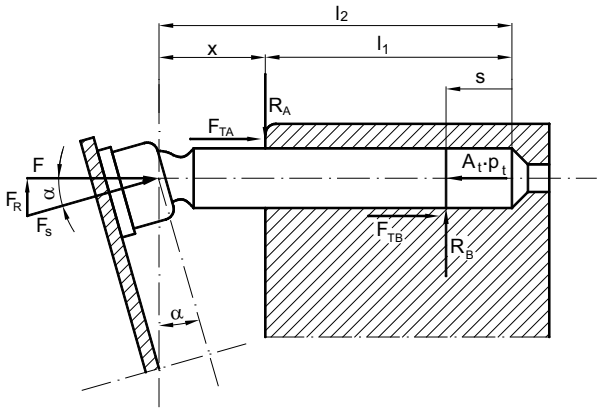

Fig. 2. Forces in the piston system represented on a plane [6]

The radial force F_R, by pressing the piston towards the cylinder, causes that the piston's position is not parallel to the cylinder and strong reactions R_A i R_B appear [11]. As a result, the friction force F_T occurs in the piston working cycle. The friction force F_T can be obtained from [6,13,20]:

$$F_T = \mu(R_A + R_B). \tag{1}$$

In the available literature, the computations of reaction forces were performed in a two-dimensional system for an extreme case, i.e. for the maximum piston displacement.

In this paper, a spatial model is employed for obtaining the reactions R_A and R_B as functions of the angle φ of the cylinder block rotation. Typically, two cases of the piston system load are considered: the discrete model [6], assuming a focused load and the analog model [19, 22], assuming a continuous load in a two-dimension system. Fig. 3 shows the discrete model of the piston system load in the three-dimensional representation. It was assumed in the model that the following forces operate: the pressure force F_p originating from the pressure, the dynamic force F_a resulting from the changes in the piston system velocity in the to-and-fro motion, the inertia force F_ω occurring due to the rotation of the piston system around the axis, the spring force F_{spr} pressing the piston system to the swash plate, the force F_{st} of the hydrostatic relief of the slipper, the friction forces between the piston and the cylinder block μR_A and μR_B, and the friction force F_{TS} between the slipper and the swash plate. R_A and R_B are reactions acting where the piston presses on the sleeve inside the cylinder block and reaction R_S is exerted by the slipper toward the swash plate.

On the basis of the distribution of forces, as shown in Fig. 3, 3 equations are formulated representing projections of the forces onto the *X*, *Y* and *Z* axes and 2 equations representing moments with respect to the *X* and *Y*, axes. All these equation are presented in a general form as:

$$\sum F_{iX} = 0, \sum F_{iY} = 0, \sum F_{iZ} = 0, \sum M_{iX} = 0 \text{ i } \sum M_{iY} = 0. \tag{2}$$

There are 5 equations and 5 unknowns: R_{AX}, R_{AY}, R_{BX}, R_{BY} and R_s. The equations were solved by means of the Cramer method [2].

Active forces occurring in the model were obtained from the formulas:

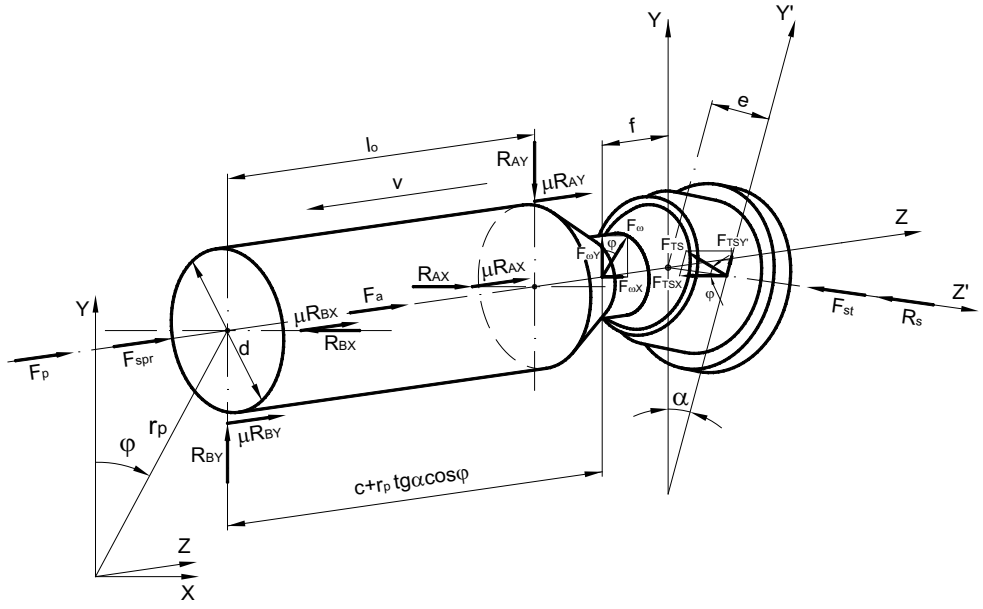

Fig. 3. Piston load in the discrete model

$$F_p = p_t \cdot \frac{\pi \cdot d^2}{4}, \tag{3}$$

$$F_{st} = C \cdot \frac{p_t \cdot \pi}{2} \cdot \left(\frac{r_{zs}^2 - r_{ws}^2}{\ln \frac{r_{zs}}{r_{ws}}} \right), \tag{4}$$

$$F_{a_i} = m_c \cdot \omega^2 \cdot r_p \cdot \mathrm{tg}\alpha \cdot \cos\varphi_i, \tag{5}$$

$$F_\omega = m_c \cdot \omega^2 \cdot r_p. \tag{6}$$

According to the Cramer method [2] the following set of equations was assumed:

$$\begin{aligned} A \cdot R_{AY} + B \cdot R_{AX} + C_i \cdot R_s &= J_i, \\ D_i \cdot R_{AY} + E_i \cdot R_{AX} + F_i \cdot R_s &= K_i, \\ G_i \cdot R_{AY} + H_i \cdot R_{AX} + I_i \cdot R_s &= L_i. \end{aligned} \tag{7}$$

The angular range ψ of the main pressure zone is treated as constant. The zone takes the range from $\frac{\alpha_m - \alpha_c}{2}$ to π (the point of departure of the cylinder block for the overlap of the valve plate) with the constant pressure p_t.

The set of equations (7) was solved by means of the Cramer formulas [2], utilizing the following expressions:

$$R_{AY_i} = \frac{R_{AY1_i}}{R_i}, \tag{8}$$

$$R_{AX_i} = \frac{R_{AX1_i}}{R_i}, \tag{9}$$

$$R_{S_i} = \frac{R_{S1_i}}{R_i}, \tag{10}$$

where

$$R_i = \begin{vmatrix} A & B & C_i \\ D_i & E_i & F_i \\ G_i & H_i & I_i \end{vmatrix}, \tag{11}$$

$$R_{AY1_i} = \begin{vmatrix} J_i & B & C_i \\ K_i & E_i & F_i \\ L_i & H_i & I_i \end{vmatrix}, \tag{12}$$

$$R_{AX1_i} = \begin{vmatrix} A & J_i & C_i \\ D_i & K_i & F_i \\ G_i & L_i & I_i \end{vmatrix}, \tag{13}$$

$$R_{S1_i} = \begin{vmatrix} A & B & J_i \\ D_i & E_i & K_i \\ G_i & H_i & L_i \end{vmatrix}, \tag{14}$$

The total reactions are:

$$R_{A_i} = \sqrt{R_{AX_i}{}^2 + R_{AY_i}{}^2}, \tag{15}$$

$$R_{B_i} = \sqrt{R_{BX_i}{}^2 + R_{BY_i}{}^2}. \tag{16}$$

In the computation model it was also assumed that the pressure variation in the upper transition zone between the suction zone and the pressure zone is linear [4] in the angular range from 0 to $\frac{\alpha_m - \alpha_c}{2}$ i.e. from 0° to 9,283° in accordance with:

$$p_j = p_s + \frac{2 \cdot (p_t - p_s)}{\alpha_m - \alpha_c} \cdot \varphi_j. \tag{17}$$

The hydrostatic force acting on the piston surface varies in accordance with:

$$F_{pj} = p_j \cdot \frac{\pi \cdot d^2}{4}. \tag{18}$$

Also, the hydrostatic relief force of the slipper varies, as below:

$$F_{stj} = C \cdot \frac{p_j \cdot \pi}{2} \cdot \left(\frac{r_{zs}^2 - r_{ws}^2}{\ln \frac{r_{zs}}{r_{ws}}} \right). \tag{19}$$

Introducing the analog model of the load of the kinematic pair piston-cylinder made it possible to calculate the load of the pair also in the spatial system. Fig. 4 shows the computation model of the analog load.

Unlike in the previously discussed model, a triangular distribution of the analog load occurring between the piston and cylinder was assumed, as discussed in [8,19,20].

In the analog model a coefficient of load transformation k was introduced (Fig. 4). The coefficient was obtained by solving Eq. (20) and taking into account the reactions R_A and R_B of the discrete model:

$$k^2 \cdot (R_B - R_A) - 2 \cdot k \cdot R_B \cdot l_0 + R_B \cdot l_0^2 = 0, \tag{20}$$

where

$$k = \frac{2 \cdot R_B \cdot l_0 - \sqrt{(-2 \cdot R_B \cdot l_0)^2 - 4 \cdot (R_B - R_A) \cdot R_B \cdot l_0^2}}{2 \cdot (R_B - R_A)}. \tag{21}$$

In the subsequent computations of the reaction to the action of the piston to the cylinder block in the analog model, Fig. 4 was used and the computation procedures adopted in the discrete model were retained.

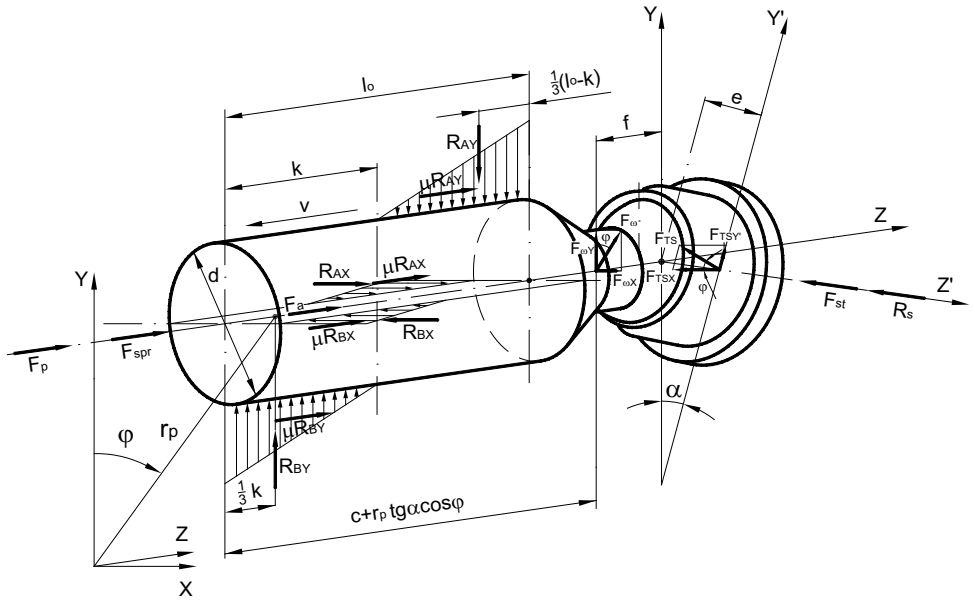

Fig. 4. Piston load in the analog model

RESULTS

The following dimensions and exploitation parameters of the pump were assumed in the calculations:

- pump pressure $p_t = 32 \times 10^6$ Pa,
- pump suction $p_s = 0$ Pa,
- shaft angular velocity $\omega = 157$ rad/s,
- central spring force $F_{spr} = 75$ N,
- total mass of the piston and slipper $m_c = 0{,}07$ kg,
- coefficient of friction between the piston and cylinder $\mu = 0{,}1$ [3],
- coefficient of friction between the slipper and the swash plate $\mu_s = 0{,}004$ [9],
- coefficient of pressure loss at the slipper $C = 0{,}9$ [4],
- swash plate inclination angle $\alpha = 16°$,
- distance between the centre of the joint to the slipper base $e = 0{,}01$ m,
- distance between the gravity centre of the slipper and piston and the piston front $c = 0{,}028$ m,
- distance between the gravity centre of the piston and slipper and the centre of the joint $f = 0{,}02$ m,
- piston diameter $d = 0{,}015$ m,
- internal radius of the slipper chamber $r_{ws} = 0{,}00498$ m,
- external radius of the slipper chamber $r_{zs} = 0{,}0101$ m,
- length of the sleeve leading the piston $l_0 = 0{,}033$ m,
- radius of the positioning of the pistons $r_p = 0{,}035$ m,
- angular coefficient of the cylinder port $\alpha_c = 26{,}109°$,
- angular coefficient of the valve plate bridge (overlap) $\alpha_m = 44{,}674°$.

As presented in Fig. 5, the values of reactions were obtained in the calculations as a function of the angle φ of the cylinder rotation in the discrete model. The values of the friction force (1) depending on the cylinder rotation angle are presented in Fig. 6.

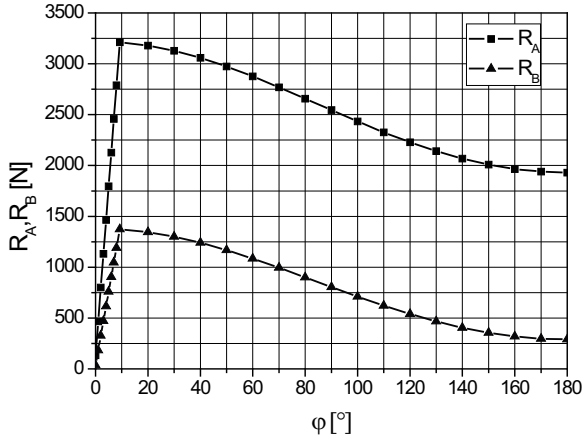

Fig. 5. Reaction as a function of the angle φ of the cylinder rotation in the discrete model

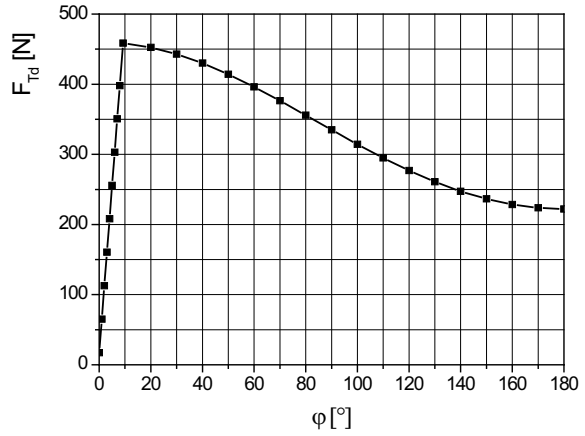

Fig. 6. Friction force F_{Td} as a function of the angle φ of the cylinder block rotation in the discrete model

On the basis of the calculations it can be observed that the friction force (1) occurring in the kinematic pair

piston-cylinder block in the pressure zone is about 4 to 8 % of the pressure force (3) in the discrete model.

Fig. 7 presents reactions in the analog model and Fig. 8 shows a comparison of the friction forces occurring between the piston and the cylinder obtained in the analog and discrete models.

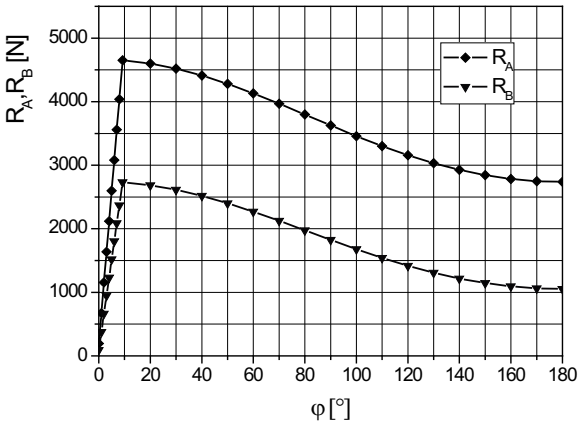

Fig. 7. Reactions R_A and R_B as a function of the angle φ of the cylinder block rotation in the analog model

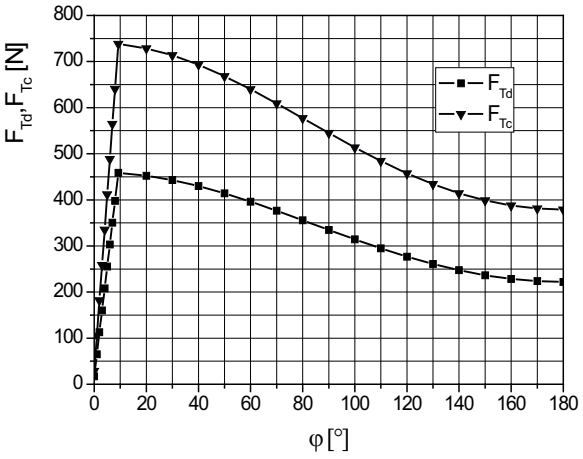

Fig. 8. Friction force F_{Tc} for the analog model and F_{Td} for the discrete model depending on the cylinder rotation angle

In the analog model the ratio of the friction force (1) to the pressure force (3) is about 7 to 13%.

CONCLUSIONS

The following conclusions can be stated on the basis of the present study:

1. The computation models of the piston load enable the assessment of friction forces and piston load depending on the cylinder rotation angle. The models can be employed for designing the kinematic pair piston-cylinder block in axial piston pumps.
2. The significantly high values of the friction force between the piston and the cylinder press the cylinder block towards the valve plate in the pump operation system and in the opposite direction in the motor operation system.
3. The analog model of the piston load is more reliable than the discrete model due to the fact that the gap height between the piston and cylinder is small.

REFERENCES

1. **Balas W.:** Łożyska hydrostatyczne w osiowych pompach tłokowych. Przegląd Mechaniczny 1966, Nr 11, 329-331.
2. **Bronsztejn I.N., Siemiendiajew K.A., Musiol G., Mühlig H.:** Nowoczesne compendium matematyki. WN PWN, Warszawa 2004.
3. **Heyl W.:** Ermittlung der optimalen Kolbenanzahl bei Schrägscheiben-Axialkolbeneinheiten. Ölhydraulik und Pneumatik 1979, 23, Nr 1, 31-35.
4. **Ivantysyn J., Ivantysynova M.:** Hydrostatic Pumps and Motors. Akademia Books International, New Delhi 2001.
5. **Jang D.S.:** Verlustanalise an Axialkolbeneinheiten. Dissertation RWTH, Aachen 1997.
6. **Kögl Ch.:** Verstellbare hydrostatische Verdrängereinheiten im Drehzahl- und Drehmomentregelkreis am Netz mit angepaβtem Versorgungsdruck. Dissertation RWTH, Aachen 1995.
7. **Kraszewski D.:** Dobieranie parametrów konstrukcyjnych łożyska hydrostatycznego o powierzchni płaskiej i sferycznej w zastosowaniu do maszyn tłokowych. Rozprawa doktorska. Pol. Wrocławska, Wydział Mechaniczny, Wrocław 1975.
8. **Murrenhoff H.:** Grundlagen der Fluidtechnik. Teil 1: Hydraulik, Shaker Verlag, Aachen 2005.
9. **Niegoda J.:** Badanie możliwości zastosowania tłoków z bezprzegubowym podparciem hydrostatycznym w pompach i silnikach wielotłoczkowych osiowych. Rozprawa doktorska. Pol. Gdańska, Wydz. Budowy Maszyn, Gdańsk 1978.
10. **Olems L.:** Berechnung des Spaltes der Kolben-Zylinderbaugruppe bei Axialkolbenmaschinen. Ölhydraulik und Pneumatik 1999, 43, Nr 11-12, 833-839.
11. **Osiecki A.:** Hydrostatyczny napęd maszyn. WNT, Warszawa 1998.
12. **Орлов Ю.М.:** Авиационные объемные гидромашины с золотниковым распределением. ПГТУ, Пермь 1993.
13. **Osiecki L.:** Badanie zjawisk zachodzących w zespole tłoczek-stopka hydrostatyczna-dławik śrubowy maszyny wielotłoczkowej osiowej. Rozprawa doktorska. Pol. Poznańska, Wydz. Budowy Maszyn i Zarządzania, Poznań 1999.
14. **Osiecki A., Osiecki L.:** Prace rozwojowe nad nową konstrukcją pomp wielotłoczkowych osiowych. Hydraulika i Pneumatyka 1998, Nr 4, 4-9.
15. **Paleczek W.:** Mathcad Professional. Akademicka Oficyna Wydawnicza EXIT, Warszawa 2003.
16. **Полозов А.В.:** Выбор оптимальных параметров объемного роторного насоса. Вестник Машиностроения 1976, № 1, 3-8.
17. **Renius K.H.:** Experimentelle Untersuchungen an Gleitschuhen von Axialkolbenmaschinen. Ölhydraulik und Pneumatik 1973, 17, Nr 3, 75-80.

18. **Renius K.H.:** Reibung zwischen Kolben und Zylinder bei Schrägscheiben-Axialkolbenmaschinen. Ölhydraulik und Pneumatik 1975, 19, Nr 11, 821-826.
19. **Ryzhakov A., Nikolenko I., Dreszer K., 2009:** Selection of discretely adjustable pump parameters for hydrualic druves of mobile equipment. Polska Akademia Nauk, Teka Komisji Motoryzacji i Energetyki Rolnictwa. Tom IX, 267-276, Lublin.
20. **Stryczek S.:** Napęd hydrostatyczny. Tom 1, WNT, Warszawa 1995.
21. **Tajanowskij G., Tanas W., 2011:** Dynamic potential of passableness of the agricultural traction-transport technological machine with a hydrodrive of wheels. Polska Akademia Nauk, Teka Komisji Motoryzacji i Energetyki Rolnictwa. Tom XIC, 306-319, Lublin.
22. **Zhang Y.:** Verbesserung des Anlauf- und Langsamlaufverhaltens eines Axialkolbenmotors in Schrägscheibenbauweise durch konstruktive und materialtechnische Maβnahmen. Dissertation RWTH, Aachen, 2000.

OBCIĄŻENIE PARY KINEMTYCZNEJ TŁOCZEK-CYLINDER W POMPIE WIELOTLOCZKOWEJ OSIOWEJ

S t r e s z c z e n i e . W pracy przedstawiono analizę obciążenia pary kinematycznej tłoczek-cylinder w pompie wielotłoczkowej osiowej. Analizę przeprowadzono z wykorzystaniem przestrzennych modeli dyskretnego i ciągłego obciążenia tloka. Określono wartości reakcji i siły tarcia występujące pomiędzy tłokiem i cylindrem dla typowej pompy wielotłoczkowej osiowej. Symulację obciążenia przeprowadzono z wykorzystaniem programu Mathcad [15].

S ł o w a k l u c z o w e : pompa wielotłoczkowa osiowa, obciążenie tłoka.